PARTIALLY GROOVED DOMAIN STABILIZATION STRUCTURES FOR VERTICAL BLOCH LINE MEMORY

R. R. Katti, J. A. Dooley, and A. Meng
Center for Space Microelectronics Technology, Jet Propulsion Laboratory,
California Institute of Technology, Pasadena, California, 91109, USA

***Abstract*--Bias field stability ranges were measured and numerically simulated for magnetic domains in garnets stabilized by partially grooved rectangular and ring grooves. Simulation results agree favorably with experimental results when finite slope effects of the groove walls are included. As bias fields increase, rectangular and ring domains both destabilize through stripe head recession. As bias fields decrease, destabilization in rectangular domains occurs by runout, while destabilization in ring domains occurs by midstripe domain buckling. While ring domains are stable at lower bias fields than rectangular domains, bias field stability ranges are approximately equal. Hence, for the same partial grooving depth, rectangular domains are preferred because they offer higher storage density potential in Vertical Bloch Line (VBL) storage arrays as long as bit propagation margins at stripe ends are sufficient.**

I. INTRODUCTION

Vertical Bloch Line (VBL) memories require the stabilization of minor loop domains in magnetic garnet materials to store data [1]. Ring domains which are wrapped around complete grooves have been investigated in previous work [2], as have rectangular stripe domains which are stabilized beneath partial grooves [3]. In this work, the bias field stability of rectangular and ring domains are both investigated when stabilized by partial grooves. Experimental data are presented which show bias field margins of rectangular and ring domains stabilized using partial grooving. Computer simulations are used to investigate straight ("flat-wall") and beveled ("sloped-wall") groove edges, and to confirm material parameters.

II. EXPERIMENTAL PROCEDURE

Nominally 2.2 μm thick magnetic garnets with compositions of $(YBiGdHoCa)_3(FeGeSi)_5O_{12}$ were used which were epitaxially grown on gadolinium gallium garnet (GGG) substrates. The magnetic parameters of the garnet included a saturation magnetization of 456 Oe, anisotropy field of 1860 Oe, zero-field stripe width of 2.36 μm, and characteristic length of 0.28 μm. Experimental chips were fabricated using ion implantation and wet etching, using a mask layout as shown in part in Figure 1. The period of the

Manuscript received February 15, 1993

grooves was 10 μm, the groove widths were nominally 1.5 μm, and the ends of the grooves were widened to conform more closely to the physical domain shapes. The implant conditions were designed to provide a groove thickness of 500 nm in the 2.2 μm-thick garnet. The regions to be grooved were first implanted with 300keV Ne^+ ions at 4 x 10^{15} ions/cm^2. The regions damaged by ion implantation were preferentially wet-etched by H_3PO_4 and HNO_3 at 110°C. After depositing a low-temperature oxide for stress relief, a chromium layer was deposited to aid magneto-optic Faraday effect domain observation in reflection. Metal layers were deposited over the mirror to provide chip functions. Sections of the wafer were diced for bias field measurements and chip characterization as SEM samples.

An inverted magneto-optic polarized-light sampling microscope was used to measure the bias field stability ranges of the magnetic domains. Nominally 5 ns light pulses at a 60 Hz repetition rate were produced from an organic dye laser at a wavelength of 590 nm light which was driven by a Sopra high-power nitrogen UV (337 nm) pulse laser. A Hamamatsu C2400 silicon-intensified-target camera and a Hamamatsu DVS-3000 image processor were used to display the images either on a monitor or VCR. A Hewlett Packard 6038A DC power supply was used to power the bias field electromagnet. Calibration of the bias field magnet was done with a gaussmeter and a sample of bubble material with a known bubble collapse field.

A small, flat 15-turn z-field coil, powered by a Hewlett Packard 214B pulse generator, was used to nucleate bubbles. The z-coil produced a pulse or oscillating magnetic field on top of the static bias field to chop the naturally occurring stripe domains. Bias field data were then obtained for rectangular domains and for ring domains, including broken rings, full rings, and semi-infinite rings.

III. SIMULATION METHOD

A previously developed two-dimensional numerical simulation [3] was used to simulate the stripe domains. A closed sequence of wall points is assumed to represent a uniform, unichiral stripe domain. Wall motion was determined by the motion of the wall points. The movement of wall points was determined by the Landau-Lifschitz-Gilbert equation which was subjected to applied fields, demagnetizing fields, an effective wall pressure, and a linear mobility subject to a coercivity and saturation velocity. The geometries of the grooves which were taken into account included flat-wall vs. sloped-wall shape, groove depth, groove width, and a uniform material thickness, as depicted in Figure 2. Several groove widths were evaluated in flat-wall simulations in order to provide a comparison for the sloped-wall simulations. A sample of the simulation output is shown in Figure 3.

Since SEM results typically showed that the groove walls had a finite slope, the simulation's calculation of the demagnetizing field from surface grooving was modified to account for the sloped walls. The degree of sloping was taken as a parameter, and the field was averaged over the thickness at each wall point.

IV. RESULTS AND DISCUSSION

Sample SEM micrographs of partial groove cross-sections from wafers 6B and 6C are shown in Figure 4. The micrographs were used to generate the simulation input data shown in Figure 2, and revealed that the grooves were not flat-walled as might be expected, but instead had relatively shallow slopes. These beveled edges are attributed to damage induced by ion scattering during implantation. The micrographs also show that the film thickness was smaller than the nominal 2.2 μm, such that in some places the thickness was as thin as 1.73 μm, with considerable variation. Because of these thickness variations, the simulations were used along with SEM results to help predict groove geometries. EDS x-ray analysis was used to confirm material composition.

Bias field measurements from wafer 6C are shown in Figure 5. Bias field simulations are also shown for sloped walls and for flat walls at three different widths. All of the experimental data shown in Figure 5 were obtained from the same stripe, to help eliminate the effects of material and processing variations. It is observed that there is significant agreement between the stripe head recession field for the sloped-wall simulation and experimental values. The field at which the stripes collapse into bubbles, however, varies considerably. This difference is presumed to be caused by the presence of varying numbers of VBLs in the experimental domains [4], induced as a consequence of the stripe nucleation process, and by the absence of any VBLs in the simulated domains. The sloped-wall simulation results were also observed to provide bias field ranges which agree with the data more closely than the flat-wall simulations. The stripe domains shown in Figure 6 in wafer 6B show similar trends.

Experimental bias field stability ranges for ring domains stabilized by ring-shaped partial grooves in wafer 6C were measured, as shown in Figure 7. When compared to Figure 5, the ring domains are seen to be stable at lower bias fields than the rectangular domains. At increasing bias fields, the destabilization mechanism for both ring and rectangular domains is the recession of the domains from the head. The destabilization mechanism at decreasing bias fields, however, is different for rectangular and ring domains. While rectangular stripe heads tend to run out from beneath the groove into the ungrooved garnet, the midstripe regions of ring domains tend to buckle. As the bias field was lowered further in these test structures, bias field stability for the ring structures was limited by the interference induced by rectangular stripes which had striped out. Thus, rectangular and ring domains in partial grooving technology were seen to have approximately the same bias field stability ranges. Simulations for complete ring domains were not performed because only simple closed domain topologies can be simulated at this time.

V. CONCLUSIONS

Bias field stability ranges were measured and numerically simulated for magnetic domains stabilized using partial grooving in magnetic garnets. Rectangular grooves and ring grooves were investigated for potential use in Vertical Bloch Line (VBL) storage arrays. Simulation results agree favorably with experimental results when finite slope effects of the groove walls are included. As bias fields increase, rectangular and ring domains both destabilize through stripe head recession from the ends of the grooves. As bias fields decrease, destabilization of rectangular domains occurs through the runout of the stripes from the grooved regions into the ungrooved garnet. Destabilization of ring domains occurs instead through midstripe domain buckling. While ring domains are observed to be stable at lower bias fields than rectangular domains, bias field stability ranges are approximately equal for partial grooves of the same depth. Thus, rectangular grooves appear preferable to ring grooves in VBL memories since they support higher storage density, as long as bias field matching occurs between minor loops and major line bubbles and bit propagation margins at stripe ends are sufficient.

REFERENCES

[1] J. C. Wu, et al., "Major Line Operation in Vertical Bloch Line Memory," *J. Appl. Phys.*, Vol. 69, No. 8,Part IIB, PP. 5754-5756, Apr. 15, 1991.

[2] P. Pougnet, et al., "Characteristics and Performance of a 1kbit Bloch Line Memory Prototype," *IEEE Trans. Magn.*, Vol. 27, No. 6, pp. 5492-5497, Nov. 1991.

[3] J. C. Wu, et al., "Partial Grooving in Vertical Bloch Line Memory," *IEEE Trans. Magn.*, Vol. 28, No. 5, pp. 2338-2340, Sept. 1992.

[4] M. Pardavi-Horvath, et al.. "Effect of ion implantation on stripe- and bubble-domain coercivity," *J. Appl. Phys.*, Vol. 59, No. 6, pp. 2119-2124, Mar. 15, 1986.

ACKNOWLEDGMENTS

The research described in this paper was carried out by the Center for Space Microelectronics Technology, Jet Propulsion Laboratory, California Institute of Technology, and was sponsored in part by the Strategic Defense Initiative Organization/Innovative Science and Technology Office, and the National Aeronautics and Space Administration. The use of the JPL/Caltech Cray for performing portions of this work is acknowledged. Dr. F. B. Humphrey is acknowledged gratefully for providing technical advice and calibration samples.

LIST OF FIGURES

Figure 1. Sample device layout of partially grooved domain stabilization structures, showing rectangular and ring domain shapes.

Figure 2. Groove dimensions used as input in sloped-wall computer simulations.

Figure 3. Simulation results showing a bubble expanding into a rectangular stripe and then running out of the groove.

Figure 4. SEM micrographs showing groove cross-sections in wafer (a) 6B and (b) 6C.

Figure 5. Bias field stability ranges. Margins (a-c) were determined experimentally for a rectangular stripe in wafer 6C. Margin (d) was simulated using sloped-wall conditions. Margins (e-g) were simulated using flat-wall conditions for groove widths of (e) 2.5 μm, (f) 1.875 μm, (g) and 1.25 μm, respectively.

Figure 6. Bias field stability ranges. Margins (a-c) were determined experimentally for a rectangular stripe in wafer 6B. Margin (d) was simulated using sloped-wall conditions.

Figure 7. (a-c) Experimental bias field stability margins for three ring domain trials in wafer 6C.

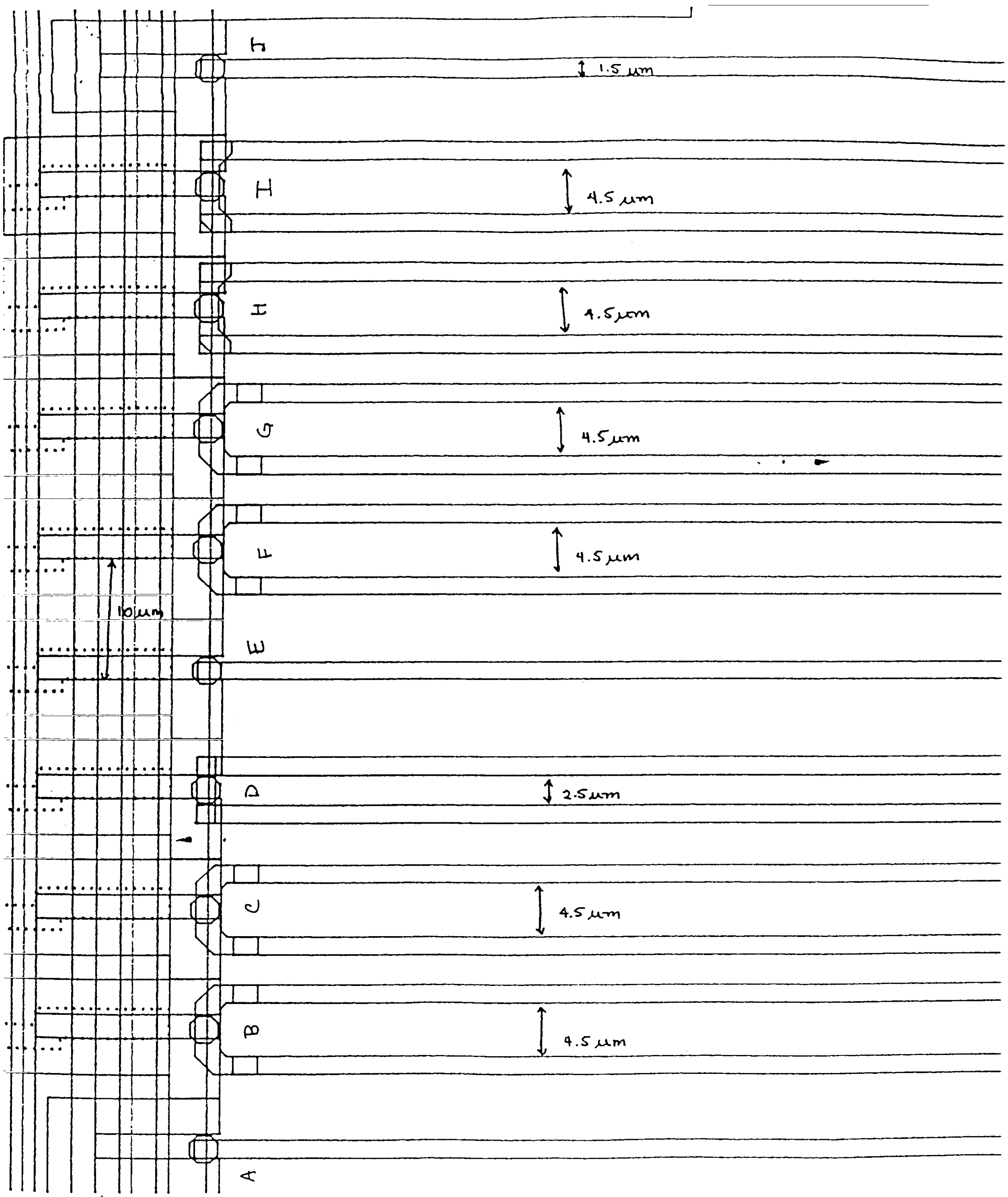

Figure 1

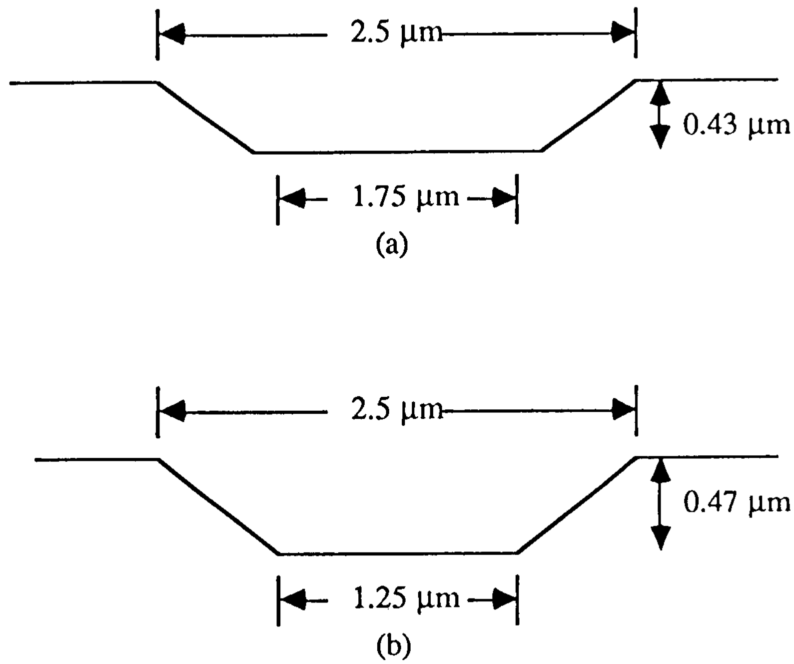

Figure 2.

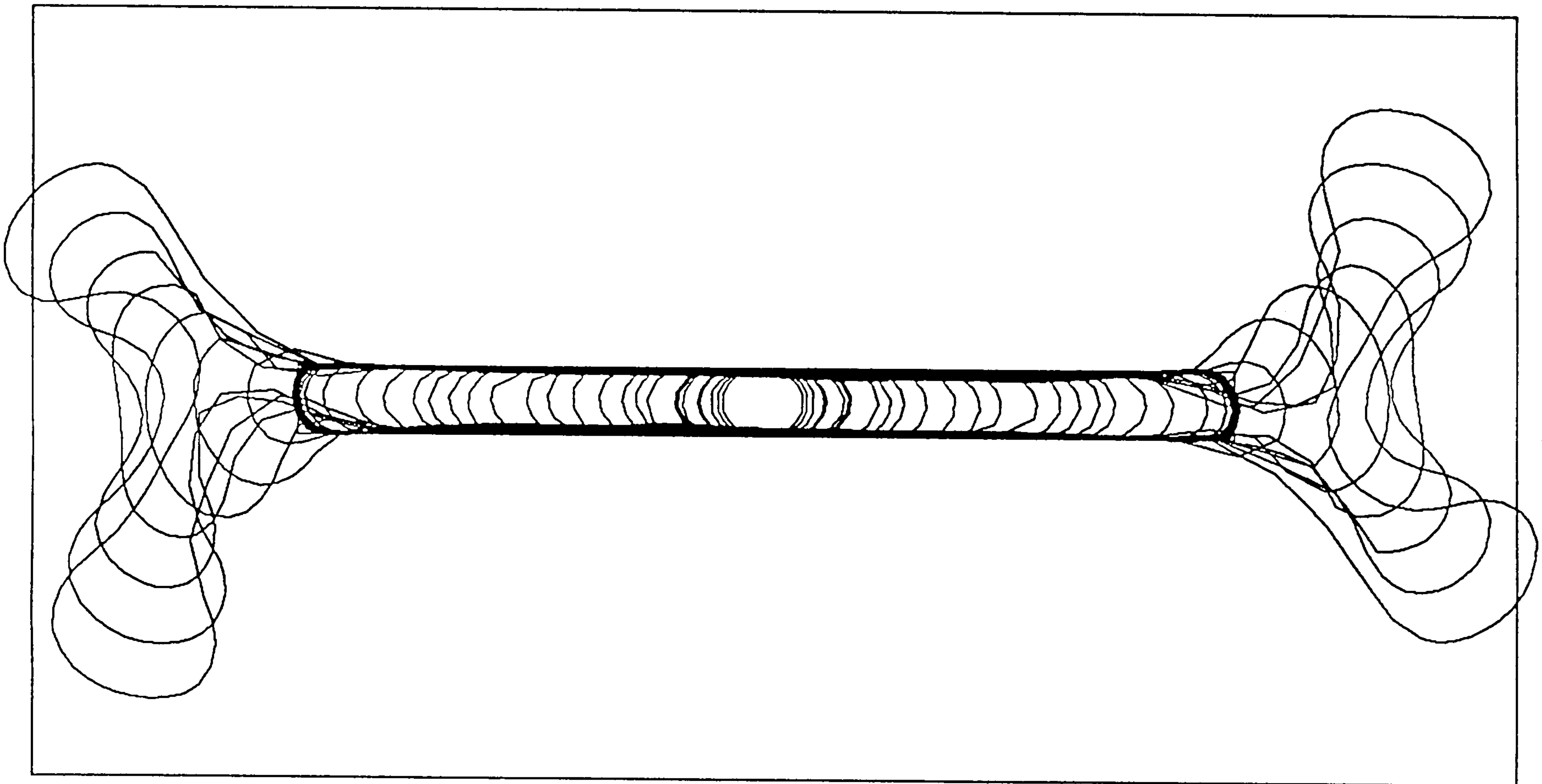

Figure 3

(a)

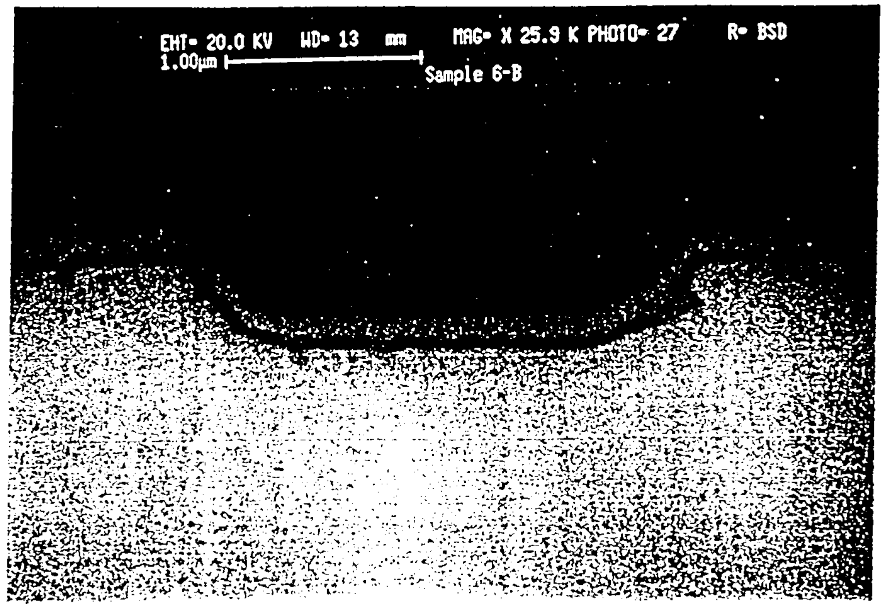
EHT= 20.0 KV WD= 13 mm MAG= X 25.9 K PHOTO= 27 R= BSD
1.00µm
Sample 6-B

(b)

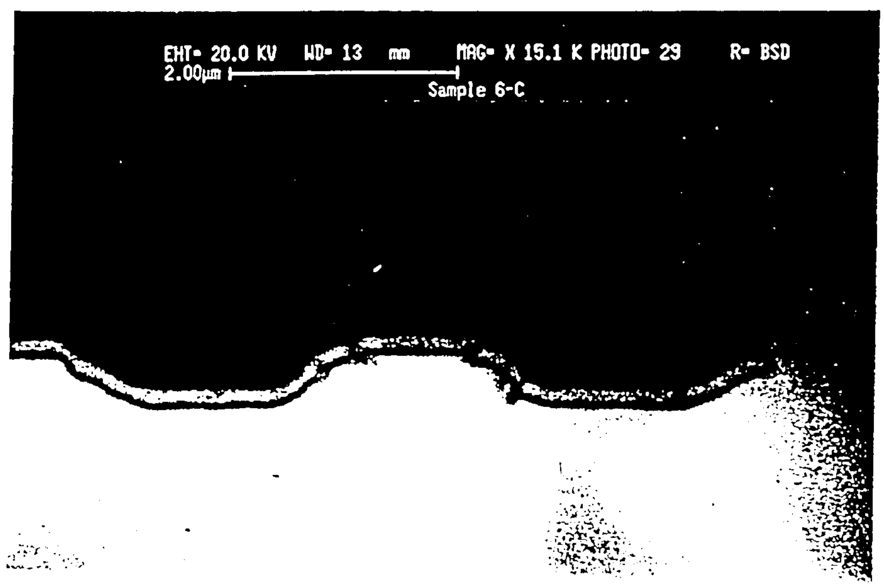
EHT= 20.0 KV WD= 13 mm MAG= X 15.1 K PHOTO= 29 R= BSD
2.00µm
Sample 6-C

Figure 1.

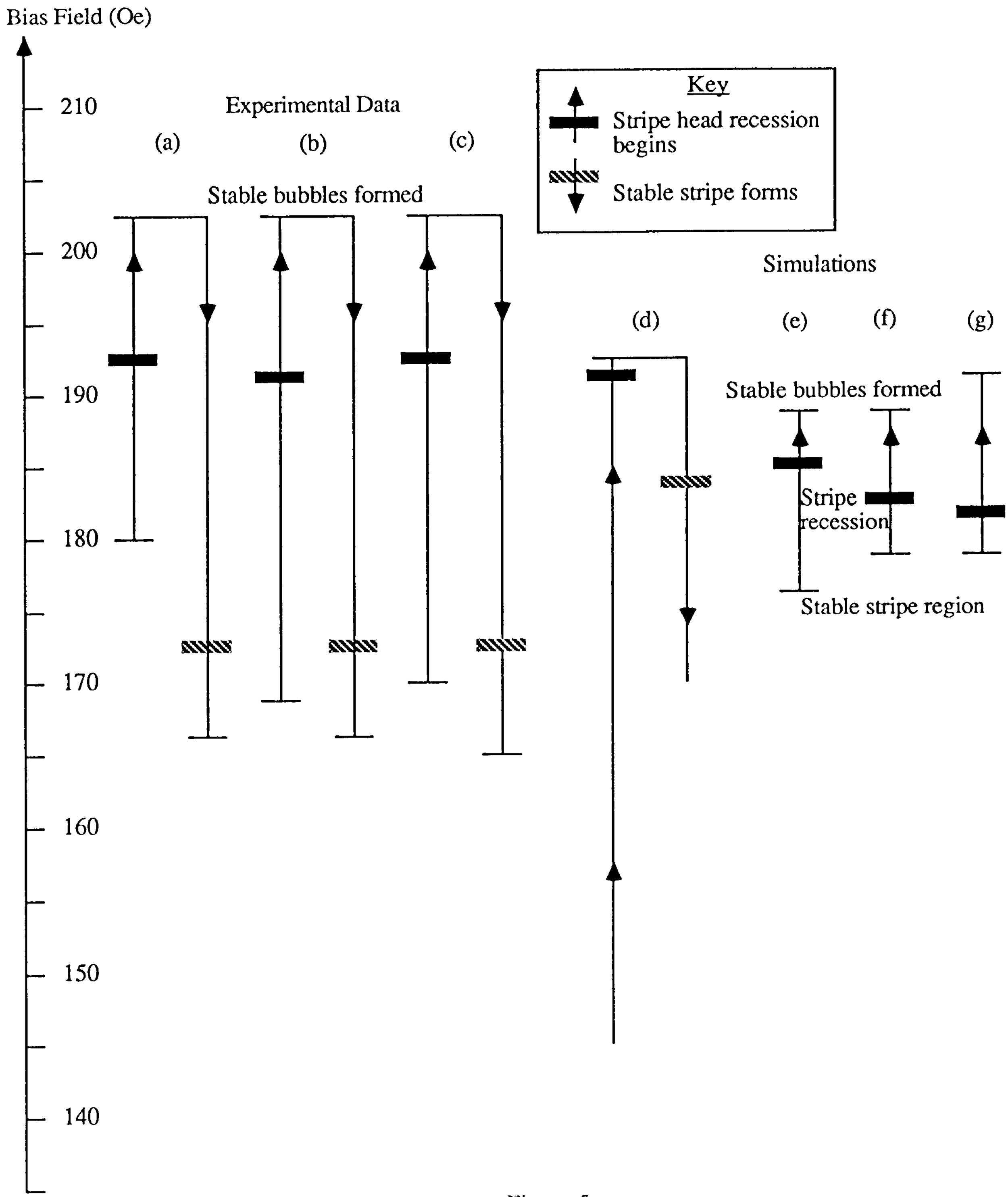
Bias Field (Oe)
210
200
190
180
170
160
150
140
Experimental Data
(a)
(b)
(c)
Stable bubbles formed
Key
Stripe head recession begins
Stable stripe forms
Simulations
(d)
(e)
(f)
(g)
Stable bubbles formed
Stripe recession
Stable stripe region

Figure 5.

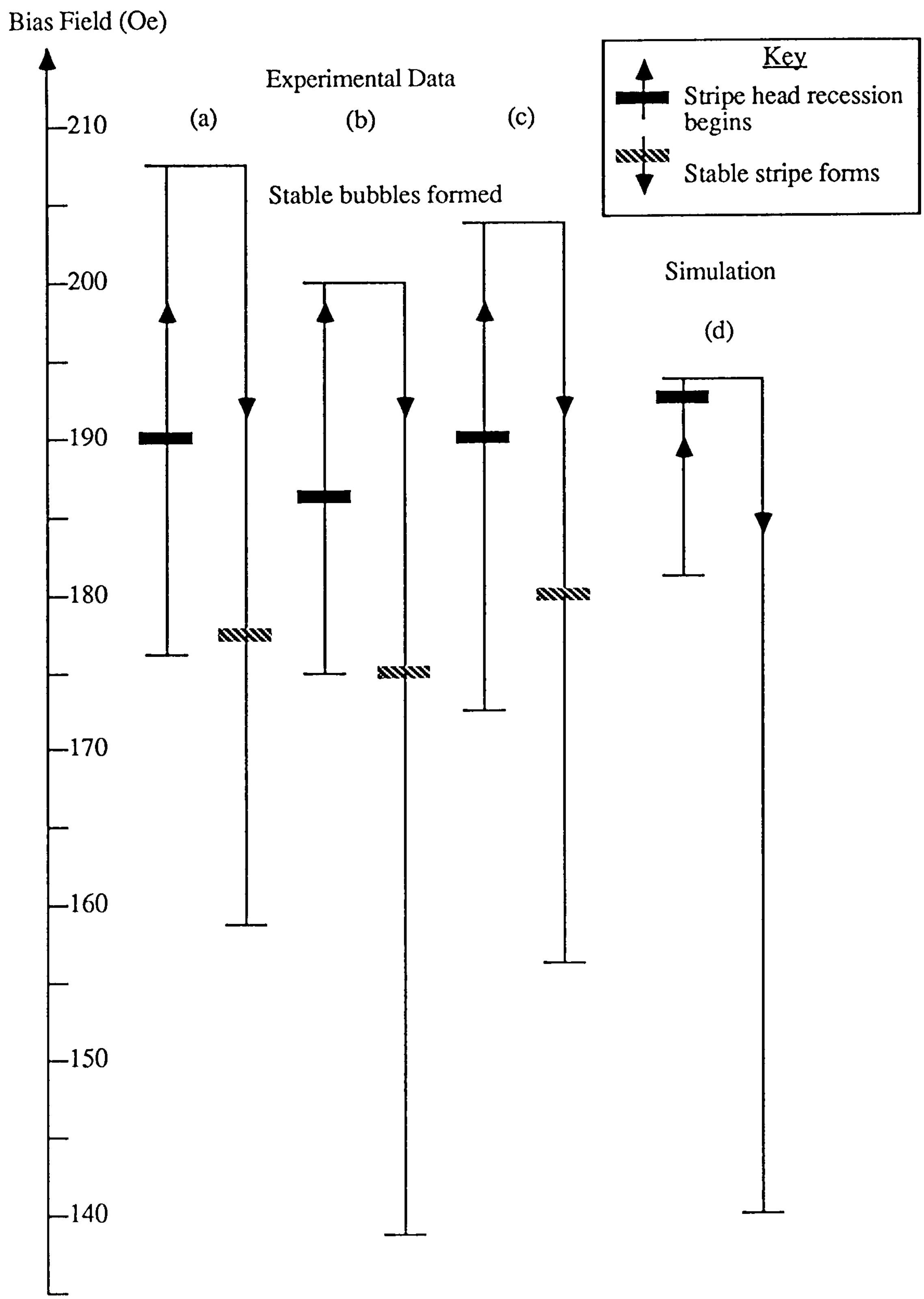

Bias Field (Oe)
210
200
190
180
170
160
150
140
Experimental Data
(a)
(b)
(c)
Stable bubbles formed
Simulation
(d)
Key
Stripe head recession begins
Stable stripe forms

Figure 6.

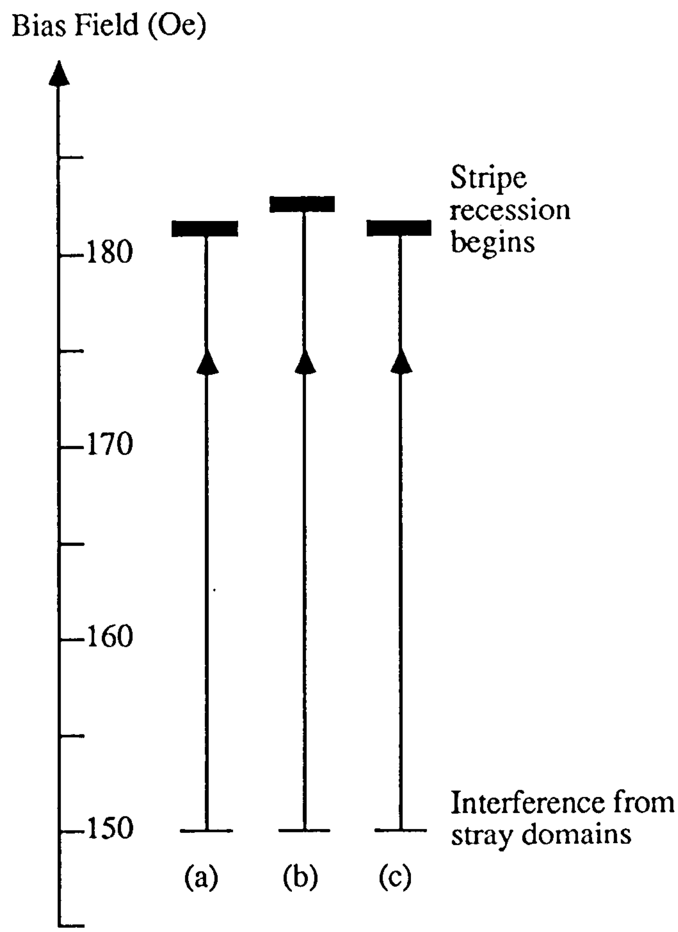
Bias Field (Oe)
180
170
160
150
Stripe recession begins
Interference from stray domains
(a)
(b)
(c)

Figure 7.